FACULTY
OF SCIENCE

Rotational Properties of Lee-Huang-Yang Bosonic Condensates from One to Two Dimensions

Hjalmar Holmström

Thesis submitted for the degree of Bachelor of Science
Project duration: 2 months, 15 hp

Supervised by Stephanie Reimann
Co-supervised by Philipp Stürmer

Department of Physics
Division of Mathematical Physics
May 2022

List of Abbreviations

- **BEC** Bose-Einstein condensate
- **GPe** Gross-Pitaevskii equation
- **MF** Mean field
- **LHY** Lee-Huang-Yang
- **HO** Harmonic oscillator
- **1D** One-dimensional
- **2D** Two-dimensional

Abstract

This thesis covers the work of a numerical examination of the rotational properties of a two-component Bose-Einstein condensate (BEC) utilizing the beyond mean-field extended Gross-Pitaevskii equation for a specified set of parameters. These parameters are chosen to cancel the strength of the mean-field interaction, which makes the system predominantly governed by the next order beyond the mean-field Lee-Huang-Yang (LHY) term. This type of BEC, referred to as an LHY-fluid, is what will be examined further in this work. The theoretical part shows how this LHY-fluid is produced with the appropriate one and two-dimensional models. These models are then utilized to quantitatively examine the rotational properties of a two-dimensional LHY-fluid in harmonic confinement and an LHY-fluid confined on a ring in one and two dimensions.

Contents

1 Introduction

A Bose-einstein condensate (BEC) is a state of matter, typically formed when a dilute gas of bosons reaches ultracold temperatures in the nK range (very close to absolute zero, which is -273.15°C or 0 K). In an ideal BEC created from a non-interacting bosonic gas, all the bosons occupy the same quantum state, making them indistinguishable and behaving coherently. This comes from the property of the boson, which allows for multiple bosons to occupy the same state (unlike fermions which are subject to the Pauli principle). The BEC was first predicted in the 1920s by Bose and Einstein [1, 2]. It was not until 1995 that the first BEC was experimentally observed [3]. This achievement was later awarded a Nobel prize in physics in 2001.

It is always challenging to model many-body systems in physics due to the sheer number of individual motions and interactions between all the constituents. This holds especially true in the typical BEC, consisting of thousands to hundreds of thousands of particles. It is, therefore, common to use approximation methods to model these systems. In the case of the BEC, the system is assumed to be very dilute and weakly interacting. This enables a mean-field (MF) description of the BEC, allowing a single common condensate wavefunction to be used instead. The usual Schrödinger equation describes the propagation with the addition of a nonlinear MF term. The MF term is dependent on the mean scattering length, which describes the interactions between the particles. This treatment of the BEC was first introduced by Gross and Pitaevskii in the 1960s [4, 5], and the equation is thus called the Gross-Pitaevskii equation (GPe).

A rotating BEC does display some exciting and non-intuitive phenomena, one of which is its superfluid property. A superfluid is fluid with no internal resistance, i.e., no viscosity. This means that after having induced a rotation in a BEC, it will (in the ideal case) keep rotating indefinitely. The usual two primary ways of stirring a BEC are using magnetic fields or rotating stirring potential (such as a laser beam). Superfluidity is also related to superconductivity, where, instead, it is an electrical current that flows without resistance. The other fact is that the rotation is "quantized", meaning that it will only exist in certain rotational quantum states. The rotation states are usually manifested as quantized vortices [6].

One should keep in mind that the GPe is an approximation of the BEC behavior. The next order correction of this approximation is commonly known as the Lee-Huang-Yang (LHY) correction, first calculated in 1957 by Lee, Huang and Yang [7]. The LHY correction is often credited with including the effects of quantum fluctuations inside the BEC. This is because it takes into account that all the collective modes are not entirely at rest (from Heisenberg's uncertainty principle), and instead undergo energy fluctuations, which are also referred to as

quantum fluctuations [8]. One interesting property of the LHY-correction is that it depends on the dimensionality of the system, unlike the MF-term.

The typical BEC containing a single species has repulsive short-range interactions and does thus form a gas. This means that unless one uses an external trapping potential, these single-species BEC are not stable and will expand over time. By using a two-species BEC, it is possible to make it self-bound, effectively making it a liquid as proposed in 2015 by Petrov [9]. This is possible by using inter-species and intra-species interactions with opposite signs. This was later experimentally tested which indeed observed self-stabilized quantum droplets [10, 11]. One should also note that the GPe cannot support droplet formation without including higher-order corrections, such as the LHY term.

For a specific condition of the interaction parameters, it is possible to completely cancel the MF interaction term in a two-component BEC, meaning that the condensate (apart from the kinetic energy) is mainly governed by the LHY-interaction term [12]. Such a condensate was successfully observed in 2021 [13]. This type of fluid is what is referred to as a LHY-fluid.

In this thesis, the rotational properties of such a LHY-fluid are investigated. This is done by analysing the ground state solutions. The analysis is done numerically using a second-order algorithm to solve the GPe under imaginary-time propagation. The algorithm used is the Fast Fourier transform, which is both accurate and converges fast. The main motivation for this thesis is to, for the first time look at the behaviour and properties of rotating LHY-fluid. In the literature, the LHY-fluid has not been investigated much further beyond the general theory and formation of it. As we will see later, the LHY-fluid does prove to have properties which are unique, compared to other types of BEC.

The following chapters of this thesis will follow the topics of the introduction. This thesis will be mainly concerned with the simulation of a pure LHY-fluid in two dimensions, but will also look at the one-dimensional case for comparison. The second chapter will introduce the main concepts of a BEC, including the LHY correction and rotational properties. The third chapter introduces the theory behind the LHY-fluid. The fourth chapter explains the method of imaginary time propagation for finding the ground states of the LHY-fluid, and lastly, chapter five and six is where the results, discussion, and conclusions of this thesis are presented.

2 General Theory of Bose-Einstein Condensation (BEC)

2.1 Bose-Einstein condensation

Simply put, a BEC is a state of matter formed by a gas of bosons at very low temperatures and densities. Two main principles allow a Bose gas to transition into this state of matter. The first is that bosons do not obey the Pauli exclusion principle, meaning that there is no restriction to the number of non-interacting bosons that can occupy the same quantum state at any time. More and more bosons will start to occupy the lowest ground state by cooling a Bose gas to temperatures close to zero. Typically, when a critical ratio of all the number of bosons is in the ground state, the gas transitions into a BEC. Secondly, when neutral gases (containing neutral atoms) are cooled, they tend to form liquids due to the van der Waals forces. To be able to observe quantum effects, the liquid state has to be avoided, which requires gases with very low densities, i.e., being extremely dilute. This is to keep the range between the bosons much larger than the range of the attractive forces between them. Also, the interparticle distance needs to be much larger than the thermal de Broglie wavelength [14, 15].

Unlike fermions, a boson is a particle with an integer spin. Any two identical bosons are symmetric under particle exchange, while fermions are antisymmetric under particle exchange. This is the characteristic trait that allows bosons to occupy the same quantum state, as we will see. The wavefunction of two bosons, one in position x_1 and the other in position x_2 as stated earlier are symmetric under position exchange, which can be expressed as

$$\Psi(x_1, x_2) = \Psi(x_2, x_1). \tag{2.1}$$

Any two body wavefunction involving two bosons with states i, j, can be constructed as

$$\Psi(x_1, x_2) = \frac{1}{\sqrt{2}}[\psi_i(x_1)\psi_j(x_2) + \psi_j(x_1)\psi_i(x_2)]. \tag{2.2}$$

Any system of N-bosons, each with their own wavefunction and assuming all are occupying the same state ψ_i, their combined wavefunction can be constructed according to

$$\Psi(x_1, ...x_N) = \sqrt{N}\prod_{n=1}^{N}\psi_i(x_n). \tag{2.3}$$

In the case of fermions such a composite wavefunction with particles in the same state cannot be formed and is thus unique for bosons. The mean expected occupation state $\langle n_i \rangle$ for a bosonic system in thermal equlibrium can be written as [16]

$$\langle n_i \rangle = \frac{1}{\exp\left(\frac{\epsilon_i - \mu}{k_B T}\right) - 1} \tag{2.4}$$

where ϵ_i is the energy level of the state i, μ is the chemical potential, k_B is the Boltzmann constant and T is the temperature of the system. As $T \to 0$, the mean expected occupation state $\langle n_i \rangle \to \langle n_0 \rangle$, which is the ground state of the system. For a BEC one can use a common condensate wavefunction $\Psi(r)$ to represent the whole system where all N-number of particles are in the ground state ψ_0,

$$\Psi(r) = \sqrt{N}\psi_0(r). \tag{2.5}$$

The normalization of the condensate can then be defined as

$$N = \int_{-\infty}^{\infty} |\Psi(\vec{r})|^2 d\vec{r}. \tag{2.6}$$

Another useful quantity is the density of the condensate, which is defined as

$$n(\vec{r}) = |\Psi(\vec{r})|^2. \tag{2.7}$$

2.2 The Gross-Pitaevskii equation (GPe)

For a system of interacting particles, deriving an exact solution becomes increasingly difficult and almost impossible for a large particle number N. Instead of finding the exact solution, approximations are due. One such approximation is the so-called MF approximation used in the GPe.

To derive the GPe, it is assumed that the space between particles is greater than their scattering length a, in the so-called dilute limit. We also need to assume that the system has very low energy, i.e that all bosons occupy the ground state, occurring at zero temperature. This allows for the replacement of the two body potential $V_{at}(r - r')$ with a pseudo-potential contact interaction using the Dirac delta function $V_0\delta(r - r')$ [8]. This is because the distance of the atomic potential becomes very small in comparison to the wavefunction of the bosons. Since the pseudo potential has zero range and can thus be considered a constant, V_0 is replaced with the coupling constant g which is related to the three-dimensional scattering constant a according to

$$g = \frac{4\pi\hbar^2 a}{m}. \tag{2.8}$$

The effective Hamiltonian for a bosonic system of N-particles, including the zero-range contact interaction, can be written as

$$H = \sum_{i=1}^{N} \left(-\frac{\hbar^2}{2m}\frac{\partial^2}{\partial \vec{r}_i^2} + V(\vec{r}_i) \right) + g \sum_{i<j} \delta(\vec{r}_i - \vec{r}_j) \tag{2.9}$$

where m is the mass of the particles and $V(\vec{r}_n)$ is an external confinement potential. The use of the Dirac-delta function makes the whole calculation much simpler. The energy functional of the system, using the condensate wavefunction Ψ becomes [15]

$$E[\Psi] = \int d\vec{r} \left(-\frac{\hbar^2}{2m} |\nabla \Psi(\vec{r})|^2 + V(\vec{r}) |\Psi(\vec{r})|^2 + \frac{1}{2} g |\Psi(\vec{r})|^4 \right). \tag{2.10}$$

The GPe can be derived using the variational approach by taking the derivative of the energy with respect to the complex wavefunction [17],

$$i\hbar \frac{\partial \Psi}{\partial t} = \frac{dE}{d\Psi^*}. \tag{2.11}$$

Inserting Eq. (2.10) into Eq. (2.11), the time dependent GPe becomes

$$i\hbar \frac{\partial}{\partial t} \Psi(\vec{r}, t) = \left(-\frac{\hbar^2}{2m} \nabla^2 + V(\vec{r}, t) + g |\Psi(\vec{r}, t)|^2 \right) \Psi(\vec{r}, t). \tag{2.12}$$

The GPe is a nonlinear Schrödinger equation where all interactions between particles are treated according to the mean-field approximation. It is important to remember one of the assumptions we made: that all particles occupy the ground state. In reality, interacting condensates are constantly depleted, meaning there will always be particles within the condensate that does not occupy the ground state. If we want to account for small amounts of depletion, then Bogoliubov theory can be used to derive a more accurate equation. In that sense, the GPe can be seen as the lowest order approximation. The next order approximation, otherwise known as the LHY-correction, is what will be discussed in section 2.4.

2.3 Two-component BEC

A two-component BEC contains two different types of bosonic species instead of one. When describing such a system, the inter-species interaction between the two different species also has to be considered. Each species is described with its own condensate wavefunction Ψ_i, with $i \in \{1, 2\}$. Both species have their own mass m_i, density n_i, coupling constant g_{ii} and particle number/normalization constant N_i such that $N_i = \int |\Psi_i|^2 d\vec{r}$. The inter-species coupling constant is symmetric, meaning that each species affects the other just as much $g_{12} = g_{21}$. The total energy of such a system is [12]

$$E[\Psi] = \int d\vec{r} \left(\sum_i -\frac{\hbar^2}{2m_i} |\nabla \Psi_i|^2 + \sum_i V_i n_i + \frac{1}{2} \sum_{ij} g_{ij} n_i n_j \right) \tag{2.13}$$

where V_i is the external potential which is usually symmetric, such that $V = V_1 = V_2$. Using the same method as in the previous section, by inserting the energy into Eq. (2.11), the GPe can be obtained. The Gross-Pitaevskii equations for each species in a two-component BEC become [18]

$$\begin{cases} i\dfrac{\partial}{\partial t}\Psi_1 = \left(\dfrac{\hbar^2}{2m_1}\nabla^2 + V + g_{12}|\Psi_2|^2\right)|\Psi_1| + g_{11}|\Psi_1|^2\Psi_1 \\ i\dfrac{\partial}{\partial t}\Psi_2 = \left(\dfrac{\hbar^2}{2m_2}\nabla^2 + V + g_{12}|\Psi_1|^2\right)|\Psi_2| + g_{22}|\Psi_2|^2\Psi_2. \end{cases} \tag{2.14}$$

For a two-component BEC, the scattering length a_{ij} for the inter- and intra-species interaction is related to the coupling constants g_{ij} according to the following relation

$$g_{ij} = \frac{2\pi\hbar^2 a_{ij}(m_i + m_j)}{m_i m_j}. \tag{2.15}$$

2.4 The Lee-Huang-Yang-correction (LHY)

In the limit of weak interactions, it is often sufficient to use the regular GPe. In the other case, when the interactions are stronger and in the pursuit of a better understanding of the dynamics of a BEC, the LHY-correction is used. As previously mentioned, the LHY-correction is the first order correction to the GPe, and is often credited to describe quantum fluctuations within the condensate. This is because it takes into account the fact that at the ground state, the condensate still undergoes zero-point energy fluctuations due to Heisenberg's uncertainty principle [8]. The GPe including the LHY-correction is what is commonly referred to as the extended GPe. For a two-component BEC, the Hamiltonian for such a system is shown below in Eq. (2.16) [14, 19]. For simplicity, it is assumed that the mass of the two bosonic species are equal ($m = m_1 = m_2$).

$$\hat{H} = \sum_{i,k}\frac{\hbar^2 k^2}{2m}\hat{a}^\dagger_{i,k}\hat{a}_{i,k} + \frac{1}{2\mathcal{V}}\sum_{i,k_1,k_2,q} g_{ii}\hat{a}^\dagger_{i,k_1}\hat{a}^\dagger_{i,k_2+q}\hat{a}_{i,k_1}\hat{a}_{i,k_2+q} + \frac{g_{12}}{\mathcal{V}}\sum_{k_1,k_2,q}\hat{a}^\dagger_{1,k_1}\hat{a}^\dagger_{2,k_2+q}\hat{a}_{1,k_1+q}\hat{a}_{2,k_2}. \tag{2.16}$$

Here, $\mathcal{V}$ stands for the volume of the system and $\hat{a}$, $\hat{a}^\dagger$ are the bosonic creation and annihilation operators. The interaction potential g_{ij} is assumed to be constant for both inter-species and intra-species interactions. The ground state of the system can be obtained by diagonalizing the Hamiltonian, which can be done by using the standard Bogoliubov theory. Replacing the creation and annihilation operators for the total number of atoms in each component and doing the appropriate canonical transformations [19, 20], the energy density functional $\mathcal{E} = E/\mathcal{V}$ becomes [14]

$$\mathcal{E} = \frac{1}{2}\sum_{ij} g_{ij}n_i n_j + \frac{1}{2}\sum_{\pm}\sum_{k}(E_\pm(k) - \frac{\hbar^2}{m}k^2 - mc_\pm^2), \tag{2.17}$$

where the first term is the MF term and the second is the LHY term. For $E_\pm(k)$ and $c_\pm^2$,

$$E_\pm(k) = \sqrt{\frac{\hbar^2}{2m^2}c_\pm^2 k^2 + \hbar^2 k^4/4} \tag{2.18}$$

$$c_{\pm}^2 = \frac{1}{2m}\left[g_1 n_1 + g_2 n_2 \pm \sqrt{(g_1 n_1 - g_2 n_2)^2 + 4g_{12}^2 n_1 n_2}\right] \tag{2.19}$$

where $c_{\pm}$ are the sound velocities, according to the Bogoliubov theory. To get the final energy correction, Eq. (2.17) is integrated over momentum space for the number of dimensions of the system. It is also worth mentioning that the MF term is not dependent on the number of dimensions of the systems unlike the LHY term, which will be shown in section 3.

2.5 Droplet formation and the three dimensional GPe including the LHY corrention

When the LHY-correction is taken into account, it becomes possible for the BEC to form a self-bound liquid droplet. This is only possible if certain requirements are met [9]. For a typical one-component BEC gas, the condensate tends to disperse rapidly if there are no external potentials containing it (see the left panel in Fig. 2.1). However, using a two-component BEC which fulfills the requirements mentioned before, it is possible to create a local minimum that enables a self-bound droplet to form (see the right panel in Fig. 2.1) [8].

The energy density of a single-component BEC in its ground state is [7]

$$E/\mathcal{V} = \frac{g}{2}n^2 + \frac{128a^{3/2}}{15}n^{3/2}, \tag{2.20}$$

where the first term is the MF term and the second is the energy contribution from the LHY correction. For a two-component system, the equation can be derived from Eq. (2.17) [19]. Assuming that the two-component system is symmetric, meaning that $n_1 = n_2 = n$, and $g_1 = g_2 = g$. The energy density then becomes

$$\frac{E_{LHY}}{\mathcal{V}} = \frac{1}{2}\delta g n^2 + \frac{256\sqrt{\pi}}{15}(n|a_{12}|)^{5/2}, \tag{2.21}$$

where $\delta g = g_{12} + g$. As can be seen, it is possible to have a negative MF term and a positive LHY term by letting $\delta g < 0$. This is attained when the intra-species interactions g and the inter-species interaction g_{12} have opposite signs, while in the case of the single-component BEC, Eq. (2.20), both the MF and the LHY term has to be either positive or negative. For most single-component BEC the interaction term is positive, meaning that it has repulsive interactions.

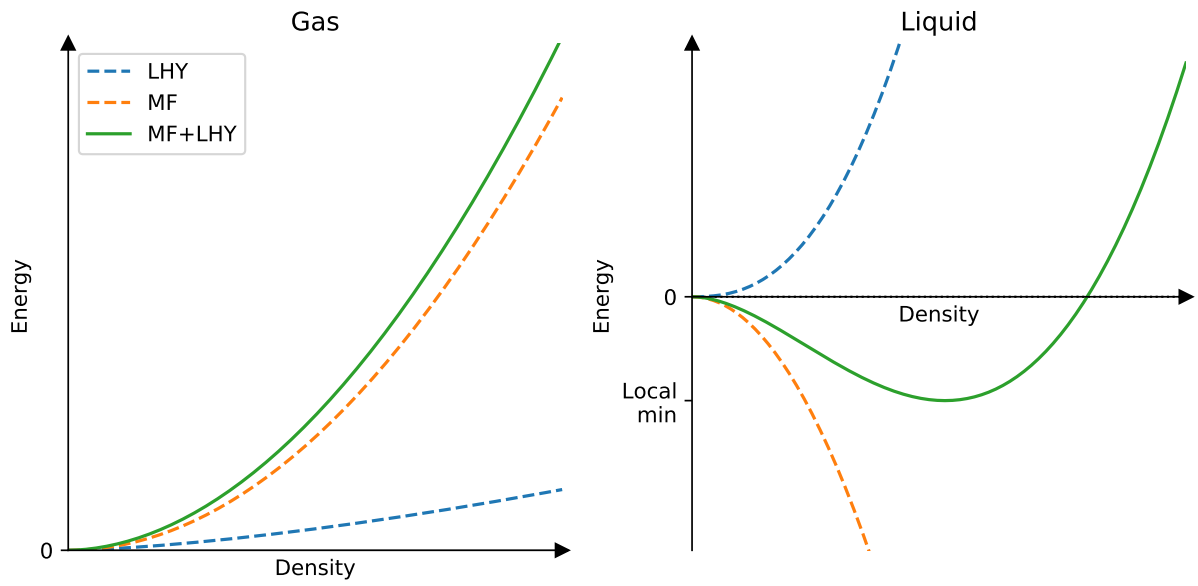

Figure 2.1: Energy vs density schematic. The blue dashed line is the energy contribution from the MF, the orange dashed line is the energy contribution from the LHY energy and the green line is the total energy. Left panel: Diagram for a typical single species BEC gas. A single species BEC is not stable and will eventually disperse. Right panel: Diagram for a two-component BEC with a repulsive MF term and an attractive LHY-correction term. The energy has a minimum for a certain density, which is created when certain conditions are met. This allows for self-bound liquid BEC droplets to from.

2.6 Quantized currents

Two main phenomena enable quantized currents (i.e. circulation states) to exist. The first is that the currents are persistent, which comes from the fact that BEC has superfluid properties and can thus remain in circulation states without experiencing any energy loss (ideal case). Such phenomena have been observed before in superfluid helium, where the currents lasted for a relatively long time [21, 22]. The other phenomenon is that these rotation states can only exist for certain energy levels. This comes from the constraint that the phase must be continuous, as will be shown later.

The dynamics of rotating BEC has been studied before [6, 23, 24, 25, 18, 26]. Generally, by inducing more and more angular momentum into the system, vortices tend to form within the condensate. It increases in number as the angular momentum increases, until a critical angular momentum is reached. Then, depending on what parameters are used the BEC tends to create one giant vortex or a large rotating ring (depending on how you look at it) [26]. This is assuming that there is some trapping potential that prevents the BEC from escaping. Vortices can also be induced in BEC droplets using the extended GPe, where the self-stabilization of the condensate prevents it from dispersing [27]. The size of the vortices is dependent on the interaction strength and the density/local density of the condensate.

Proceeding with introducing the theory, first taking a look at the theory behind quantized currents and then taking a look at the energy of such a system. Starting with the time-dependent wavefunction $\Psi(r,t)$, a typical condensate wavefunction can always be written as [28, 18]

$$\Psi(r,t) = \sqrt{n(r,t)}\exp\left(\frac{iS(r,t)}{\hbar}\right), \tag{2.22}$$

where S is the phase. Deriving from the concepts of ordinary fluid mechanics and using current density defined from quantum mechanics, one can define the superfluid velocity v_s as

$$v_s = \frac{\hbar}{m}\nabla S. \tag{2.23}$$

The fact that the velocity depends on the phase is the reason that the current becomes quantized. The integral of the phase along a closed contour in space must be an integer multiple of 2π. Where n_w is an integer number called the winding number.

$$\Delta S = \oint \nabla S \cdot dl = 2\pi n_w \tag{2.24}$$

As one can see, since the phase S has to be continuous, any circulation around an axis must therefore be quantized. This means that the velocity can only exist in specific quantized circulation states,

$$v_s = \frac{2\pi\hbar}{m} n_w. \tag{2.25}$$

These quantized circulation states are obviously not the ground state of the system. If there exist stable circulation states, then they must correspond to some metastable configuration with a local energy minimum [29]. The dispersion relation offers insight into how such local energy minima are formed. The energy of a 1D single-component rotating BEC in a ring under the constraint of fixed angular momentum is shown in Fig. 2.2 [18]. This type of behaviour has been demonstrated before in various BEC in 1D, 2D and 3D [18, 27, 29, 30].

The 1D dispersion relation can be understood by analysing the energy functional. Some of the general features of the 1D dispersion relation was proved by Bloch [31]. The energy $E(L)$, as shown below, contains two parts, one envelope part which is proportional to L^2 and one periodic part $e(L)$. The periodic part $e(L)$ has the periodic property $e(L + N\hbar) = e(L)$ and is symmetric around $L = 0$ such that $e(-L) = e(L)$.

$$E(L) = \frac{L^2}{2Nm} + e(L) \tag{2.26}$$

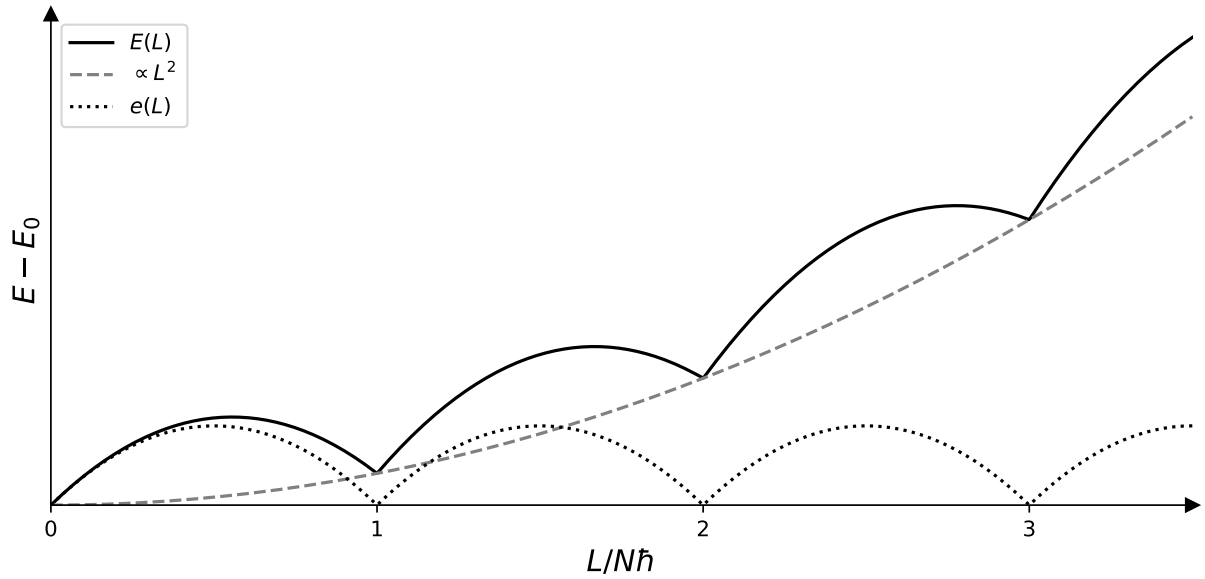

Figure 2.2: The figure shows the theoretical dispersion relation (using the regular GPe, Eq. (2.12)) for a 1D one-component BEC in a ring for fixed values of angular momentum. The total energy is a combination of one parabolic part proportional to L^2 (dashed) and one periodic part (dotted). The number of local minima that exists depends on the relative size of the two terms.

As can be seen in Fig. 2.2, it is the periodic part that is responsible for creating a local minimum and is minimized for integer values of $L/N\hbar$. The periodic part appears due to the internal interactions of the condensate [18]. However, a local minimum is not always a given and will only appear when the periodic energy contribution is sufficiently large compared to the quadratic part.

3 Lee-Huang-Yang (LHY) Fluid

3.1 Formation of a LHY-fluid

The definition of a LHY-fluid is that it is a liquid BEC that is mainly governed by the LHY-correction term. This requires that the MF term becomes much weaker than the LHY-correction term or that it is completely canceled. This can be done using a two-component BEC. The requirement needed to cancel the MF term is that $g_{12} = -\sqrt{g_{11}g_{22}} = -g$ or $a_{12} = -\sqrt{a_{11}a_{22}}$ [12]. Why this is the case is easy to see, the MF energy density is $\frac{1}{2}\sum_{ij} g_{ij}n_i n_j$ [from Eq. (2.17)] and for the symmetric case ($n = n_1 = n_2$ and $g = g_{11} = g_{22}$) it becomes $g_{12}n + gn = \delta g n$. The strength of δg is proportional to the MF potential and using the requirement this term becomes zero, canceling the MF term. What is left is a pure LHY-fluid, which is indeed also what has been observed in a recent experiment (2021) [13].

It is also worth noting that for the non-symmetric case, apart from the requirement mentioned previously, it is also necessary to choose atom numbers such that $N_2/N_1 = \sqrt{g_{11}/g_{22}}$. The condensate wave function takes the form $\Psi_2 = \Psi_1(g_{11}/g_{22})^{1/4}$, which for $g_{11} = g_{22}$ are equivalent $\Psi = \Psi_2 = \Psi_1$ [12]. For the rest of this thesis, only the symmetric case will be considered and therefore only the first requirement has to be accounted for, which in this case becomes $g_{12} = -g$. Also, all proceeding equations will use natural units such that $\hbar = m = 1$. Inserting these conditions in Eq. (2.19), the sound velocities become

$$c_{\pm}^2 = gn \pm gn \Longrightarrow c_+^2 = 2gn \quad \text{and} \quad c_-^2 = 0. \tag{3.1}$$

Inserting into Eq. (2.17), the energy density functional for a LHY-fluid becomes (for simplicity $c_+ = c$)

$$\mathcal{E} = \frac{1}{2}\sum_k \left(\sqrt{\frac{k^4}{4} + k^2c^2} - \frac{k^2}{2} - c^2 \right) \tag{3.2}$$

which will be used to derive the 1D and 2D energies for the LHY-correction term in the next two chapters.

3.2 LHY-fluid in one dimension

Proceeding from the last section, the 1D energy density from the LHY-correction is calculated by taking the 1D integral over momentum space. The 1D energy density from the LHY-correction becomes, using Eqs. (3.2)-(3.1) [32]

$$\mathcal{E}_{\text{LHY1D}} = \frac{-4\sqrt{2}}{3\pi}(gn)^{3/2}. \tag{3.3}$$

In the presence of a trapping potential V, Eq. 3.3 can be utilized using the local density approximation, which allows $n \to |\Psi(n)|^2$. The total energy is then

$$E[\Psi] = \int dx \left(-\frac{1}{2}\frac{\partial^2}{\partial x^2}|\Psi(x)|^2 + V(x)|\Psi(x)|^2 - \frac{4\sqrt{2}}{6\pi}g^{3/2}|\Psi(x)|^3 \right). \tag{3.4}$$

The extended GPe for a 1D LHY-fluid can then be derived using Eq. (2.11),

$$i\frac{\partial}{\partial t}\Psi(x,t) = \left(-\frac{1}{2}\frac{\partial^2}{\partial x^2} + V(x) - \frac{\sqrt{2}}{\pi}g^{3/2}|\Psi(x,t)| \right)\Psi(x,t). \tag{3.5}$$

As seen in the equation above, the 1D potential from the LHY-correction is negative and is thus an attractive potential, meaning that the condensate tends to increase in density. However, a collapse is avoided by the zero point kinetic energy, which can stabilize the system. It is also assumed that the particle count does not exceed a critical number or the condensate is not a uniform gas where quantum pressure is absent, in which case the condensate is otherwise unstable [17]. The concept of quantum pressure is somewhat similar to that of classical pressure. When applying the quantum mechanical description to particles constrained in a region of space, the kinetic energy tends to increase as the volume decreases.

3.3 LHY-fluid in two dimensions

Similar to the 1D case, the 2D energy density from the LHY-correction is calculated by taking the 2D integral over momentum space. In two dimensions, this integral is divergent. To avoid this problem, a cutoff κ is introduced [14]. Using Eqs. (3.1)-(3.2), the energy density becomes (see appendix for the derivation)

$$\mathcal{E}_{\text{LHY2D}} = \frac{g^2}{2\pi}n^2 \ln\left(\frac{2g\sqrt{e}}{\kappa^2}n\right). \tag{3.6}$$

The coupling constant g is related to the two-dimensional scattering length a_{2D} by

$$g = \frac{4\pi}{\ln\left(\epsilon/\kappa^2\right)}, \tag{3.7}$$

where $\epsilon = 4e^{-2\gamma}/a_{2D}^2$, and γ is Euler's constant. By introducing a new auxiliary energy parameter Δ it is possible to define a new coupling constant $\tilde{g}$ such that $\tilde{g} = \frac{4\pi}{\ln(\epsilon/\Delta)}$. The coupling constant g is related to $\tilde{g}$ according to

$$g = \tilde{g} + \frac{\tilde{g}^2}{4\pi}\ln\left(\frac{\kappa^2}{\Delta}\right) + \mathcal{O}(\tilde{g}^3). \tag{3.8}$$

Substituting g for $\tilde{g}$ in Eq. 3.6, the new expression for the energy density becomes

$$\mathcal{E}_{\mathrm{LHY2D}} = \frac{\tilde{g}^2}{2\pi} n^2 \ln\left(\frac{2\tilde{g}\sqrt{e}}{\Delta} n\right), \tag{3.9}$$

which is no longer dependent on the cutoff κ. Making sure that κ^2/Δ is not exponentially large, the two coupling constants g and $\tilde{g}$ are approximately equivalent $g \approx \tilde{g}$, which allows the two coupling constants to be used interchangeably [14, 29]. The energy can be calculated by taking the integral over the 2D space, which becomes

$$E[\Psi] = \int d^2r \left[-\frac{1}{2}|\nabla\Psi(r)|^2 + V|\Psi(r)|^2 + \frac{g^2}{2\pi}|\Psi(r)|^4 \ln\left(\frac{2g\sqrt{e}}{\Delta}|\Psi(r)|^2\right)\right]. \tag{3.10}$$

The extended Gpe for a 2D LHY-fluid can then by derived, similarly as in the last section

$$i\frac{\partial}{\partial t}\Psi = \left[-\frac{1}{2}\nabla^2 + V + \frac{g^2}{\pi}|\Psi|^2 \ln\left(\frac{2ge}{\Delta}|\Psi|^2\right)\right]\Psi. \tag{3.11}$$

Analyzing the shape of the 2D energy contribution from the LHY-correction, one can see that it does form a local minimum, which allows for self-bound droplets to form. However, this only occurs for low densities, at high densities the 2D LHY-fluid behaves like a regular repulsive gas.

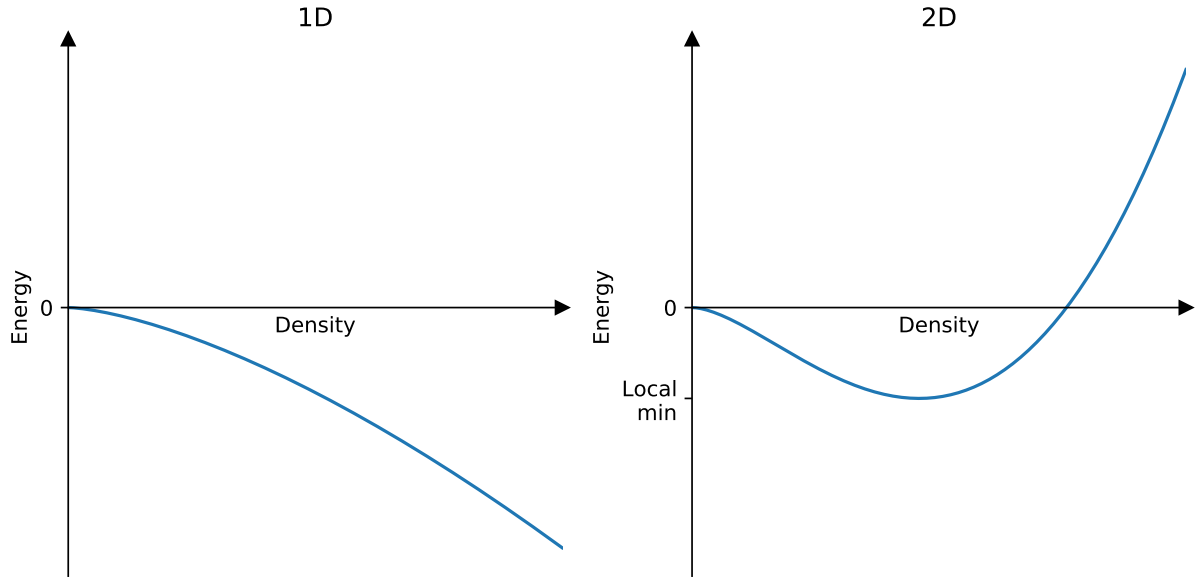

Figure 3.1: Comparison between the 1D and 2D LHY energy contribution terms, from Eqs. (3.4)-(3.10). Compared to the 1D LHY energy contribution, the 2D LHY energy contribution does from a local minimal which allows for self-bound droplets to form. This is similar to the graph in Fig. 2.1 (right graph), but here the 2D droplet is stabilized by the LHY-correction only. Also worth noting that, this minimum only occurs for low densities, but for higher densities the 2D LHY term is positive (which is usually the case in potential confinements with a high particle count).

4 Numerical Solution of the GPe

4.1 Trapping confinement in a rotating frame

For the numerical work of this thesis, we will look at a BEC in four different types of confinements. For the two-dimensional case, we will use a harmonic trap and a ring confinement consisting of a harmonic trap with a central Gaussian, see Fig. 4.1. In two dimensions, the dimensionless form of the extended GPe for a LHY-fluid, Eq. (3.11), will be used. Adding the trapping potential, the full equation for a LHY-fluid in a rotating frame with angular frequency Ω becomes

$$i\frac{\partial}{\partial t}\Psi = \left[-\frac{1}{2}\nabla^2 + \frac{1}{2}(\omega_x^2 x^2 + \omega_y^2 y^2) + V_0 e^{-(x^2/\mu_x^2 + y^2/\mu_y^2)} + |\Psi|^2 \ln(|\Psi|^2) - \Omega L\right]\Psi, \tag{4.1}$$

For symmetrical traps, as will be used in section 5.1 and section 5.2, $\omega = \omega_x = \omega_y$ and $\mu = \mu_x = \mu_y$. The Gaussian trap strength V_0 is chosen according to $V_0 = 0.2\mu^{3/2}$, using μ as a parameter. In the case of the elliptic ring confinement, $\omega = \omega_x$ $\omega/2 = \omega_y$, $\mu = \mu_x$ and $\mu/2 = \mu_y$.

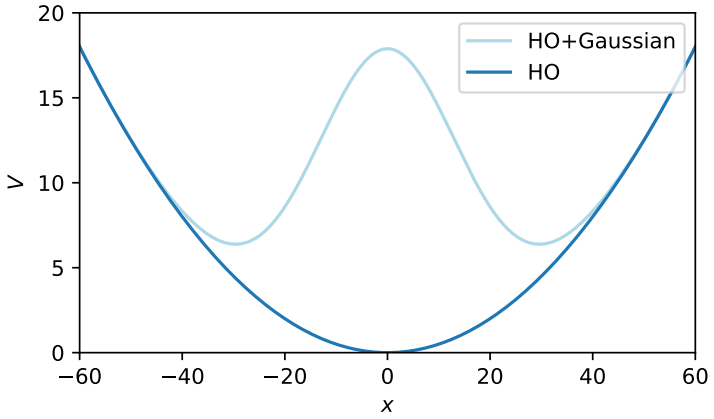

Figure 4.1: Two different confinement potentials. The dark blue line shows a harmonic potential while the light blue is a harmonic potential with the addition of a central Gaussian potential, from Eq. (4.1).

In one dimension, a ring trap can effectively be made by having periodic boundary conditions in the system. The dimensionless form of extended GPe for a 1D LHY-fluid, from Eq. (3.5) is

$$i\frac{\partial}{\partial t}\Psi = \left[-\frac{1}{2}\nabla^2 - \beta|\Psi|\right]\Psi \tag{4.2}$$

where $\beta = \frac{\sqrt{2}}{\pi} g^{3/2}$ will be used as a parameter to modulate the strength of the LHY term. A two-component dimensionless form of the regular GPe under symmetric conditions becomes, using Eq. (2.14)

$$i\frac{\partial}{\partial t}\Psi = \left[-\frac{1}{2}\nabla^2 + \alpha|\Psi|^2\right]\Psi \tag{4.3}$$

where $\alpha = \frac{1}{2}\delta g$, will similarly be used as a parameter to modulate the strength of the MF term.

4.2 Imaginary time propagation

When studying the dynamics of a quantum mechanical system, the wavefunction can be iterated forward in time using real-time propagation. Real-time propagation can be expressed using the standard time evolution operator,

$$\Psi(t) = \exp\Big(-it\hat{H}\Big)\Psi(0). \tag{4.4}$$

But, if we want to find the ground state solution of a quantum mechanical system, the imaginary time propagation is a great tool to use. In this method, the real-time t in the real-time propagation is replaced with imaginary time τ, such that $\tau = it$. Essentially, it works by "projecting out" the ground state of any quantum mechanical superposition. Why this works can be easily seen when the wavefunction is expressed as a superposition of all the eigenstates,

$$\Psi(t) = \sum_i \exp(-\tau E_i) c_i \psi_i \tag{4.5}$$

where c_i are the coefficients and ψ_i is the eigenvector for each state. For increasing values of τ, the larger E_i is, the faster the eigenstate decays (goes to zero). This means that for large τ only the eigenstate with the lowest energy will remain, i.e. it converges to the ground state. The Hamiltonian of our system, depending on the number of dimensions d is shown in Eq. (4.6) below, which should correspond to Eq. (3.5) and Eq. (3.11) for a 1D and 2D system respectively. Where T_i is the kinetic energy, V_i is the external potential and U is the nonlinear term in the GPe,

$$\hat{H} = \sum_i^d (T_i + V_i) + U = T + U. \tag{4.6}$$

The wave function is then iterated forward in imaginary time via

$$|\Psi(\tau + \Delta\tau)\rangle = e^{\Delta\tau(T+U)}\,|\Psi(\tau)\rangle\,. \tag{4.7}$$

Convergence of the imaginary time iteration can be assessed by monitoring the chemical potential or the energy of the system. To solve the extended GPe for a 1D or 2D LHY-fluid, the numerical method from the following paper referenced here [33] is used. It is essentially an algorithm for iterating the imaginary time propagation using the fast Fourier transform method.

5 Results and Discussion

5.1 Quantized vortices

In our investigation of the rotational properties of a pure 2D LHY-fluid, we begin by looking at one of the simplest cases, a BEC droplet inside a rotating harmonic trap, see Eq. (4.1) and Fig. 4.1. Here we look at the ground states for different rotational frequencies, using imaginary time propagation, as introduced in section 4.2 to find the ground states. What we find is similar to what has been observed before in other cases using the GPe and extended GPe [29].

As the rotational frequency increases, vortices are induced inside the BEC. The number of vortices in the rotational ground states grows as the rotational frequency increases. Fig. 5.1 shows the density distributions for different rotational ground states for up to seven vortices and Fig. 5.2 shows the phases of the corresponding rotational ground states. As can be seen in these figures, the vortices are positioned in a way such that they are symmetrically distributed along the symmetry axis.

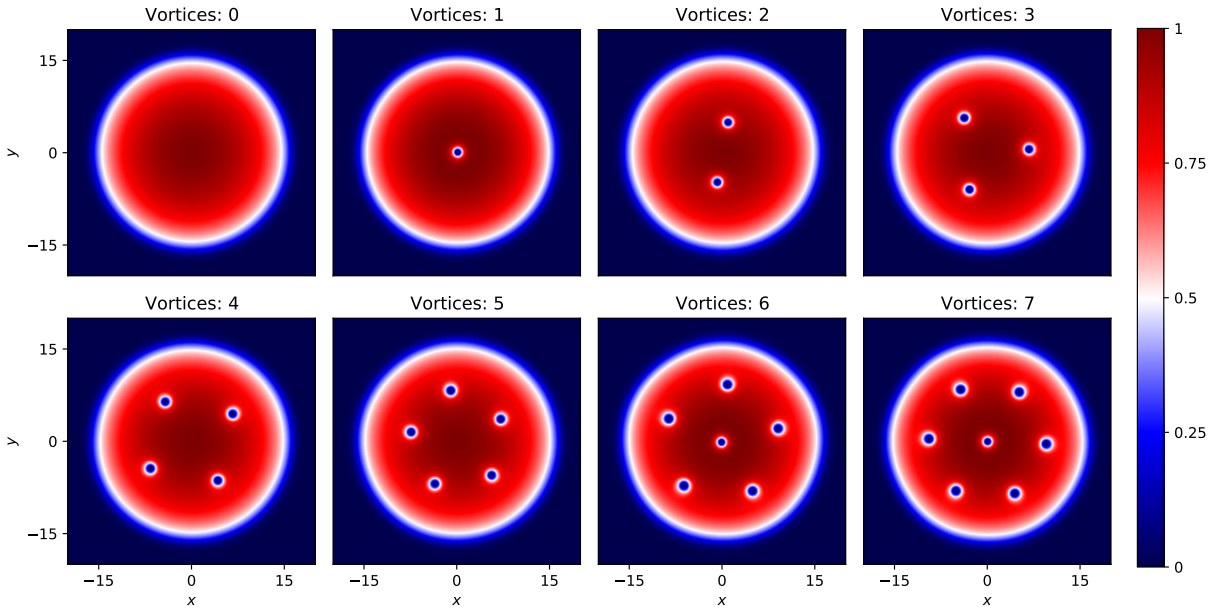

Figure 5.1: Density distribution of the rotational ground states for different rotational frequencies Ω in a harmonic trap ($V_0 = 0$) with $\omega = 0.1$ and $N = 1000$. For increasing values of the rotational frequency Ω, the energy level of the rotational ground states are quantized according with the number of vortices inside the droplet. The colorbar represents the relative density distribution from zero to one (one being the maximum density for each individual case). The x and y axis shows the distance in each dimension using dimensionless units.

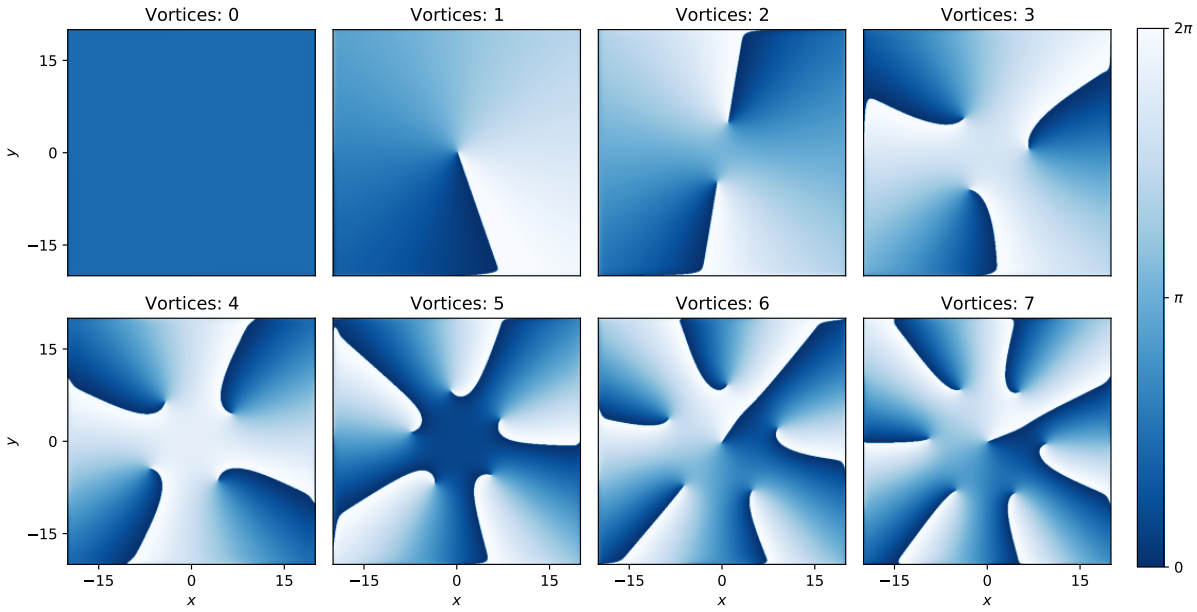

Figure 5.2: The corresponding phases of the rotational ground states from Fig. 5.1. The circulation of the phase around a point indicates the center of a vortex.

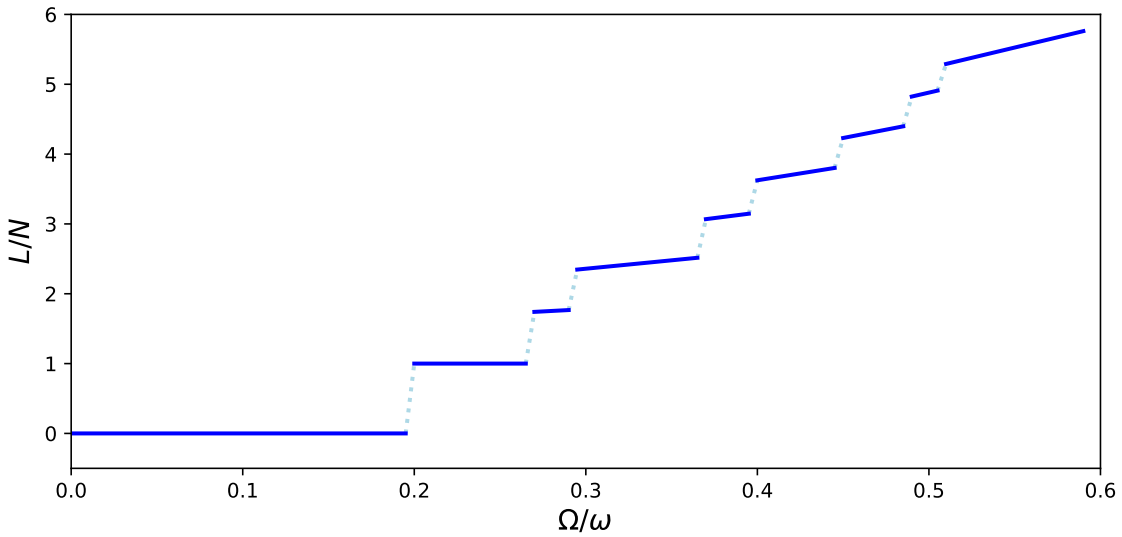

Figure 5.3: The rotational frequency Ω/ω is plotted against the angular momentum of the BEC. As can be seen in the graph, the angular momentum of the states are separated into distinct "lines" which corresponds to the different rotational ground states, starting with zero vortices at $\Omega/\omega = 0$.

Fig. 5.3 shows the rotational ground state angular momentum as a function of the rotational frequency Ω/ω, for states shown in Fig. 5.1. As can be seen in the figure, the values are segmented into several parts, corresponding to the number of vortices of the state. For states that have more than one vortex, the symmetry is broken and the states can thus occupy a range of possible angular momentum values, as seen in Fig. 5.3. In practice, this is possible by letting the spacing between the vortices vary.

5.2 Rotating ring in 2D

In this section we look at a 2D LHY-fluid, confined in a ring shape potential consisting of a harmonic and Gaussian potential, see Fig. 4.1. This creates a trap that gives the condensate a ring shape as seen in Fig. 5.4. For certain thicknesses and parameters, it is possible to induce non-central vortices along the ring, but in this section, we are only interested in the case where the ring has unitary flow i.e. flows in a single direction with respect to the central axis (similar to the 1D case), which requires that the ring is sufficiently thin. The confinement potential is therefore chosen such that it is no longer possible to induce non-central vortices.

Similar to the case in the previous section (section 5.1), when the rotational frequency increases, the condensate orders itself into distinct rotational ground states corresponding to the number of circulations of the phase, which can be seen in Fig. 5.5. Due to the symmetry being conserved for all rotational states, the angular momentum appears in these fixed integer values of angular momentum. This is why in Fig. 5.6 we see these straight lines which correspond to the different rotational states.

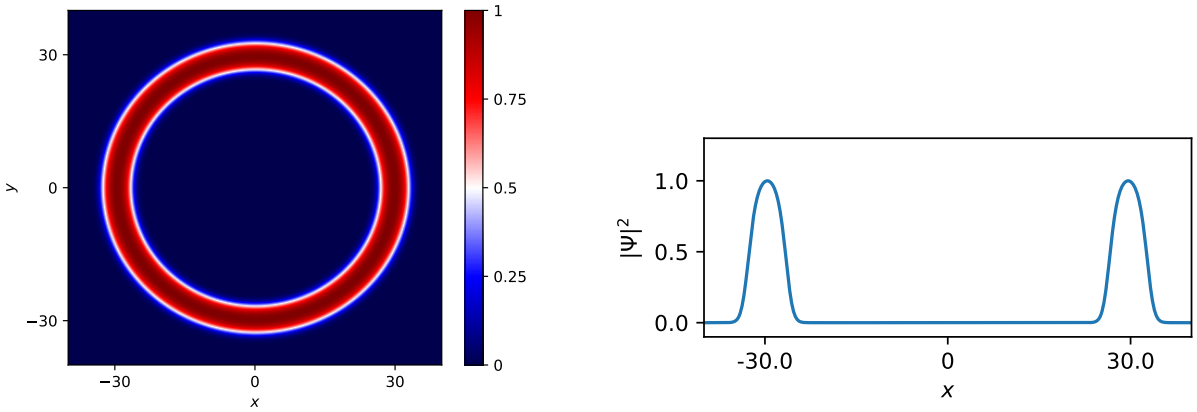

Figure 5.4: Left: Density distribution of the ground state of the LHY-fluid inside a ring trap constructed by a harmonic oscillator trap with a central gaussian function, see Eq. (4.1), $N = 1000$, $\mu = 20$. Right: Cross section of the ring density distribution at $y = 0$.

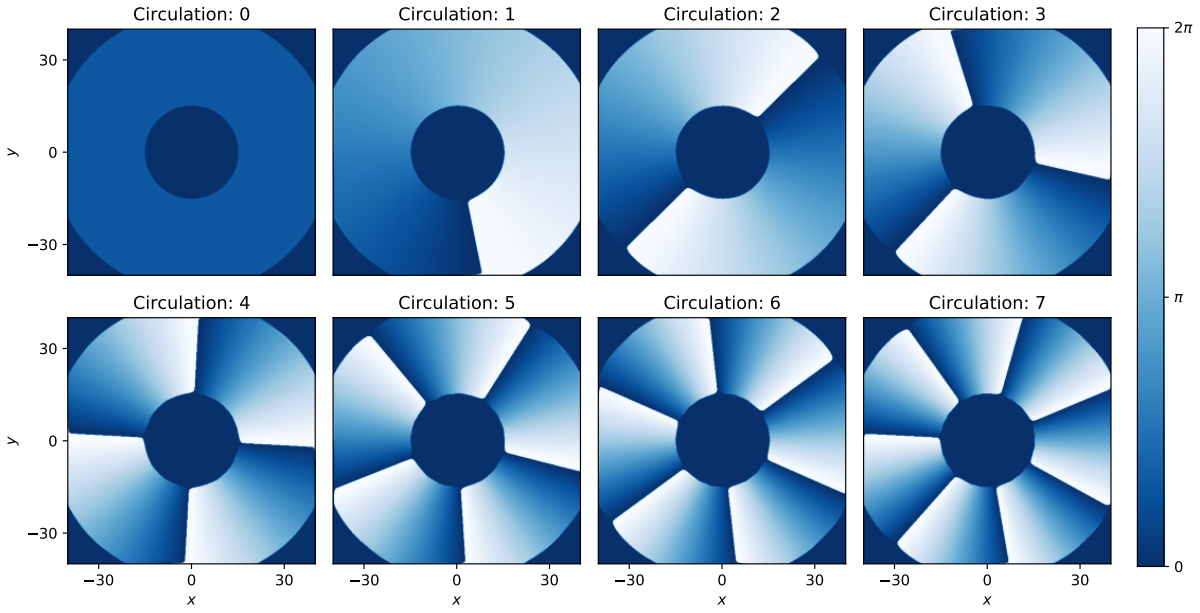

Figure 5.5: Phases of the rotational ground states for different rotational frequencies Ω, from the setup shown in Fig. 5.4. As can be seen in this figure, the rotational states are quantized according to the number of phase circulations. The phases are only calculated in the proximity of the density distributions, hence the ring shape of the phases.

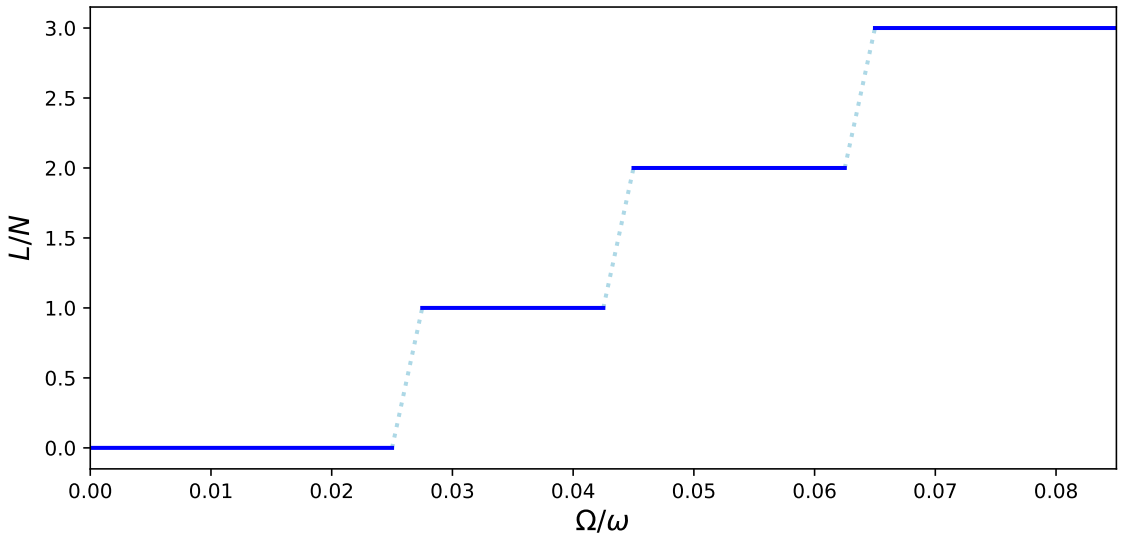

Figure 5.6: Similar plot as in Fig. 5.3. The rotational frequency Ω/ω is plotted against the angular momentum of the ring shaped condensate. As can be seen in the graph, the angular momentum has fixed values and is quantized according with the number of circulations, as shown in Fig. 5.5.

Taking a look at the energy of the ring-shaped LHY-fluid as a function of angular momentum, we end up with the graph shown in Fig. 5.7. This graph resembles the one shown in section 2.6, and can clearly be seen to consist of one periodic part and one parabolic part proportional to L^2. What is interesting about this is that this shows that even after the rotation has been induced, the currents will keep persisting in their given metastable position. This is different from the case in section 5.1, where the rotational states for the droplet are only stable while the rotation is still active. Plotting the same type of relationship for the droplet would in fact reveal no metastable points [29, 27]. Fig. 5.8 shows the specific solutions at different values of angular momentum from the graph in Fig. 5.7. The gap in density in Fig. 5.8 shows the entry of a vortex into the ring.

When we instead take a look at the same ring confinement but with a different particle count $N = 20$, the behavior of the LHY-fluid changes completely. Instead of a homogeneous ring, a (bright) soliton-like density distribution is formed which circulates inside the ring confinement, see Fig. 5.9. This is what we would expect, recalling from section 3.3 (see Fig. 3.1), that for low densities the 2D LHY-fluid interaction term becomes negative (attractive). Due to this new shape, the metastable points which existed for the homogeneous ring have disappeared. This is as expected because the density distribution is now localized in a small region in space and does not have the same constriction of the phase as the homogeneous ring does.

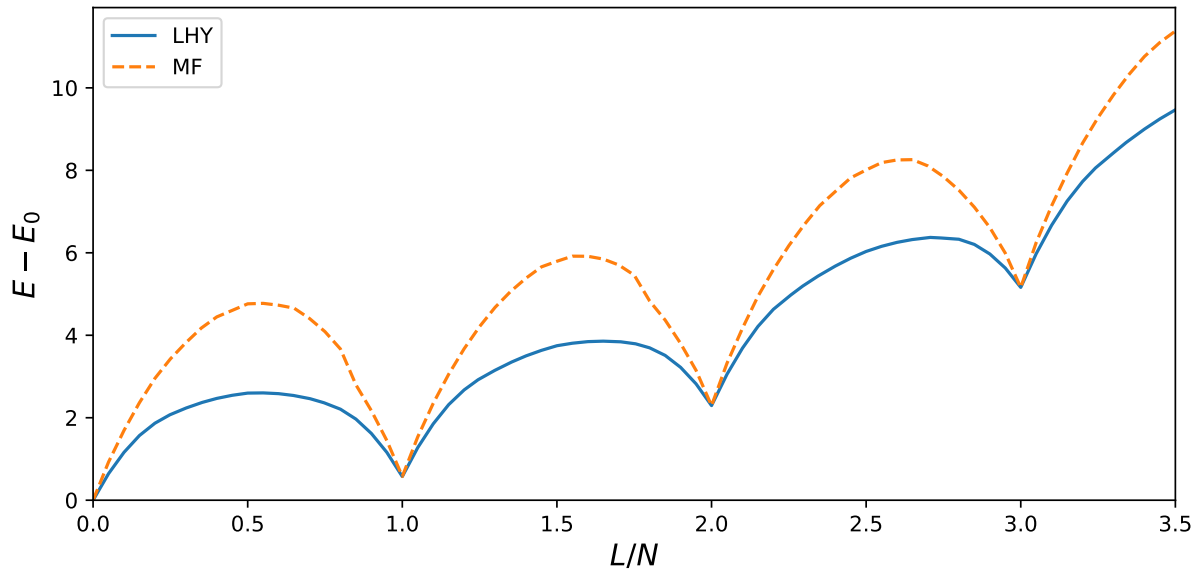

Figure 5.7: Ground state energy in the laboratory frame as a function of the angular momentum. The same system is used as shown in Fig. 5.4. The graph is made up of two parts, one periodic and one parabolic, proportional to L^2. This forms multiple local minima which can support persistent current, even if the rotation is turned off. The shape of the LHY-fluid is compared to the regular GPe solution for a two-component system where the only nonlinear term is the MF term.

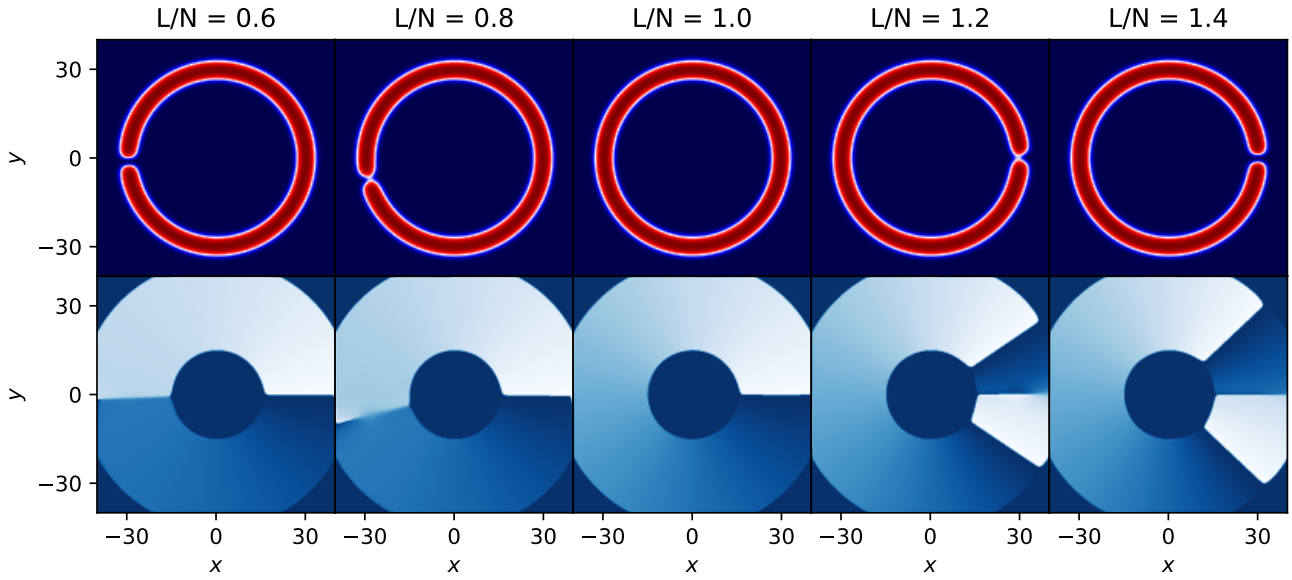

Figure 5.8: Density distribution and the corresponding phase for the ground state solutions at different angular momentum from Fig. 5.7. For solutions between the integer number of angular momentum, a tiny vortex is created to carry the excess angular momentum and can be seen "entering" the ring when approaching an integer number of angular momentum.

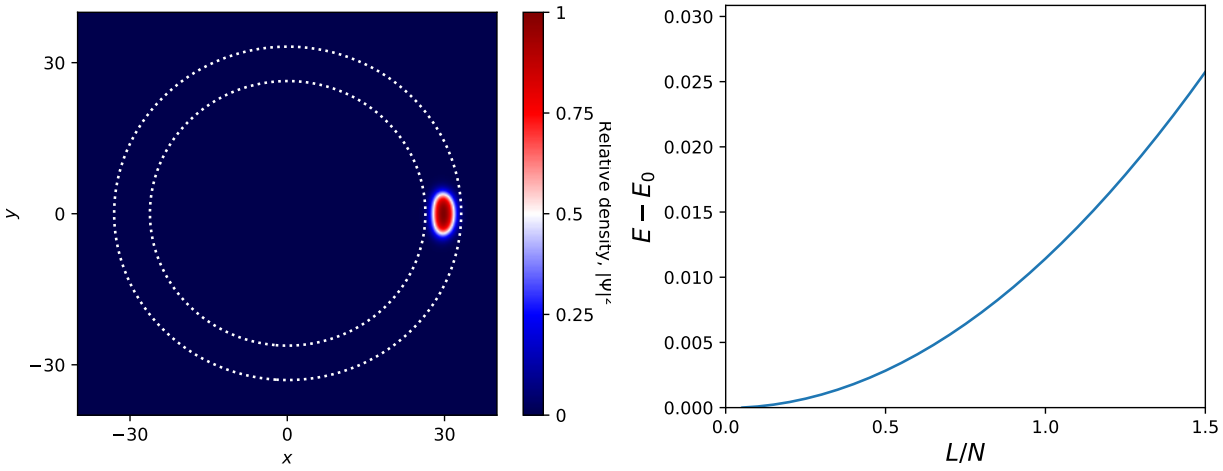

Figure 5.9: Left: LHY-fluid with $N = 20$, inside the same ring confinement as in Fig. 5.4 where the white dotted lines show the contour of the ring shaped LHY-fluid from the same figure. As can bee seen, the LHY-fluid at low densities forms a bright soliton-like density distribution. Right: Energy vs angular momentum. The graph forms a simple parabolic curve which, compared to the case shown in Fig. 5.7, has no periodic part and does thus not form any metastable minima.

5.3 Rotating ring in 1D

The next step is to compare our findings in 2D with the 1D case. Using Eqs. (4.2)-(4.3) (with $\alpha = 5$ and $\beta = 5$), we look at the energy for specific values of the angular momentum for a periodic system. In this case, we will look at both the effects of the MF term and the LHY term. Fig. 5.10 shows the energy as a function of the angular momentum for the two different models. In the MF case, using Eq. (4.3), the graph looks like the one in Fig. 5.7 and similarly allows for metastable persistent current to exist. However, for the LHY case, Eq. (4.2), no local minima are present, except at $L/N = 0$.

The reason for this difference can be seen in Fig. 5.11, which shows the solutions for different values of angular momentum. For the pure MF case, for integer values of angular momentum L/N the density of the solution is homogeneous. For angular momentum values which are not equal to an integer, the solutions form a dip with a local minimum that changes depending on the angular momentum. At a first glance this might be mistaken for a dark soliton but what we actually see is the sign of a vortex entering the ring, similarly as in Fig. 5.8. While for the pure LHY case, the negative (attractive) LHY term makes the condensate form a localized density distribution.

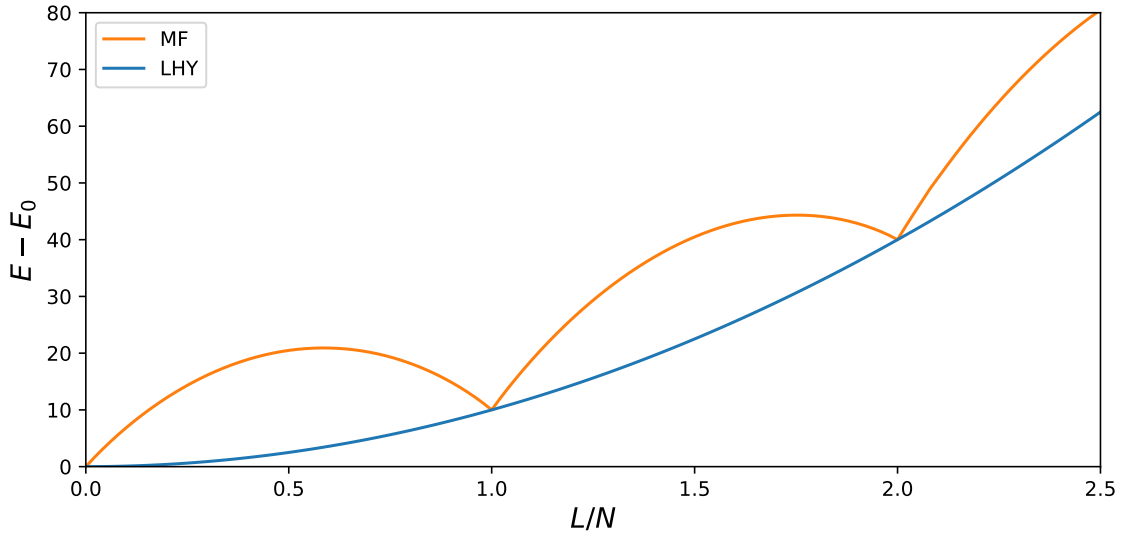

Figure 5.10: Ground state energy in the laboratory frame as a function of the angular momentum for a 1D BEC. The system are modelled with Eqs. (4.2)-(4.3) and the parameters used are $N = 20$, $\alpha = 5$ and $\beta = 5$. As can be seen, the MF solution, Eq. (4.3), forms these metastable points, as seen in Fig. 5.7 earlier, while the same does not hold true for the LHY solution, Eq. (4.2).

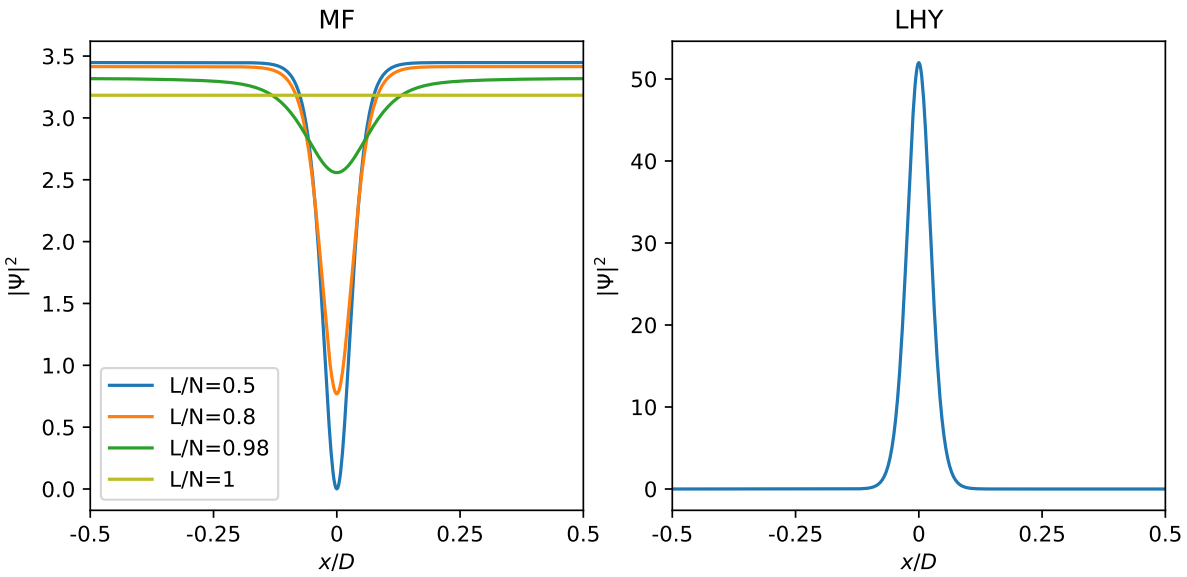

Figure 5.11: Two types of solutions from the plot shown in Fig. 5.10. D is the total length of the x-axis. Left: MF case. Between integer angular momentum states, for example $0 < L/N < 1$, the solutions form a "dip" which has its lowest minimum at half-integer angular momentum values, in this case $L/N = 0.5$. The cause of the dip is actually a vortex entering the ring, similar to the case in Fig. 5.8. Right: LHY case, the solutions have all identical shapes and forms a soliton-like density distributions.

5.4 Symmetry breaking in an elliptic Ring

In practice, it may be experimentally impossible to create a perfect ring, so by examining how a elliptical ring behaves, we are actually studying a more realistic case of the ring confinement. In the elliptic case, using the elliptic ring confinement from Eq. (4.1), it is only the ground state without any rotation that is evenly uniform along the elliptic ring trap. As the rotation frequency Ω is increased, the density tends to distribute itself more on the outer edges of the trap, see Fig. 5.12. This is reminiscent of the classical way matter tends to distribute itself in rotating systems. By changing the trap from a circular ring to an elliptic ring, the symmetry has been broken which enables the condensate to distribute itself non-evenly along the trap for a nonzero rotation frequency, which effectively makes the states lose their degeneracy, as can be seen in Fig. 5.13.

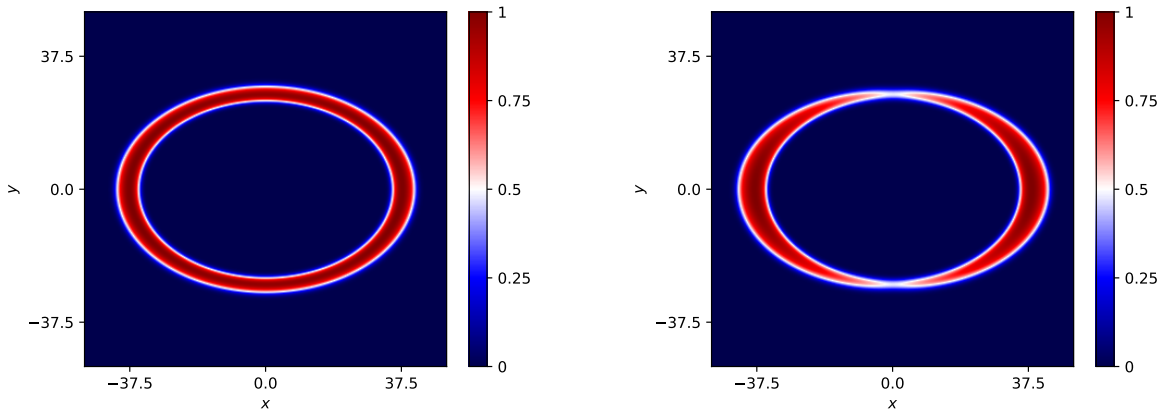

Figure 5.12: Figure shows two solutions of the rotational ground state densities, which demonstrate the shape deviation for increasing rotational frequency Ω (right) from the homogeneous density distribution (left) as consequence of the elliptical shape. Left: Ground state density at no rotation. Right: Rotational ground state density at a high rotational frequency.

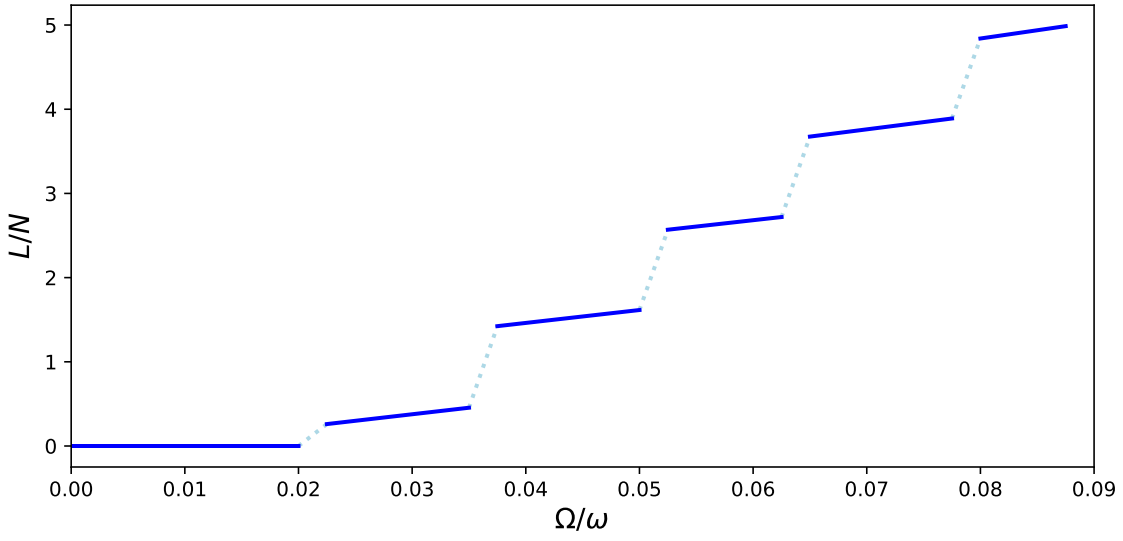

Figure 5.13: The rotational frequency Ω is plotted against the angular momentum of the ellipse shaped condensate. As can be seen the graphs, compared to Fig. 5.6, the angular momentum states are no longer straight and parallel to the x-axis.

6 Conclusions and Outlook

To conclude this thesis, we have introduced the main theoretical framework to create and model an LHY-dominated fluid, i.e. a two-component BEC modeled with the extended GPe using a specific set of parameters such that the MF term gets canceled and only the non-linear LHY-correction term remains. The remaining part of this work has been dedicated to numerically (using imaginary time propagation) investigating the rotational properties of the 2D and 1D LHY-fluid. What we find displays some new phenomena which occurs for a LHY-fluid in 1D and 2D, which is different form regular BEC.

Specifically, we have looked at the rotational behavior of an LHY-fluid in a droplet and on a ring. In the droplet (confined in a harmonic trap), as the rotational frequency increases, the angular momentum manifests as quantized states with a certain integer number of vortices. This is as expected and similar to all the other cases using one or two-component BEC with the regular or extended GPe. In the ring case, the angular momentum is manifested as quantized circulation around the ring (or multiple central vortices), which is also similar to the 1D case. It is also clear from these examples that the angular momentum states are highly dependent on the shape of the BEC and will lose their degeneracy if the symmetry is broken.

Perhaps the most interesting case is the energy vs. angular momentum relation of the 1D and 2D LHY-fluid in a ring. Firstly, when comparing the 2D LHY-fluid with the 1D MF BEC, we find points of metastable persistent current. In both cases, the nonlinear term is positive (repulsive). If we look at the 1D LHY-fluid, there are no longer any metastable points and does instead form a simple parabolic shape because the condensate instead forms a soliton-like density distribution due to the nonlinear term being negative (attractive). Secondly, for both the 1D case, and low density 2D case for a LHY-fluid in a ring, a soliton-like structure is formed which does not form any metastable points and is very different from the regular MF case.

There are two potentially exciting topics to investigate further. The first one is to investigate the transition in a ring system between 1D and 2D; how does the ring lose its metastable minima? How thin or thick does the ring need to be to still be able to support persistent metastable current? What does the LHY term look like in quasi-1D? The second one is since we know that it is possible to have self-bound LHY droplets in 2D [27], is it possible to find similar metastable currents after inducing a vortex in a weak ring-shaped potential confinement? After which the confinement potential reduces to zero after a specific time (both the trap confinement and the rotational frequency)?

Acknowledgements

I would like to sincerely thank all the people who have helped me realize this project. First off, I would like to give a special thanks to my supervisor Stephanie Reimann, for her continuous support and enthusiasm during this whole project. I also want to thank my co-supervisor Philipp Stürmer for his patience in answering lots of questions and for support regarding the numerical part of this project. Lastly, I would like to thank Koushik Mukherjee, who has been a great help in matters relating to the theoretical part of this thesis.

For people outside the department, I want to thank all of the members of my family, especially my parents who have always shown unwavering support in all of my endeavors. I would also like to thank all of my close friends who have made this time more enjoyable, with a special thanks to my friend Amir, for his support during this project.

Appendix: Derivation of the energy density for the 2D LHY-fluid

Starting from Eq. (3.2), the 2D energy contribution is derived as follows. Since the integral is divergent we will instead introduce a cutoff κ when integrating over the momentum space.

$$\mathcal{E} = \frac{1}{2}\frac{1}{(2\pi)^2}\int_{-\kappa}^{\kappa} dk \int_0^{2\pi} d\theta \left(\sqrt{\frac{\hbar^2 k^4}{4m^2} + \hbar^2 k^2 c^2} - \frac{\hbar^2 k^2}{2m} - mc^2\right) k. \tag{6.1}$$

To make the calculation less messy, we will use natural units $m = \hbar = 1$. Simplifying the above equation, it then becomes

$$\mathcal{E} = \frac{1}{4\pi}\int_{-\kappa}^{\kappa} dk \left(\sqrt{\frac{k^6}{4} + k^4 c^2} - \frac{k^3}{2} - kc^2\right). \tag{6.2}$$

For $\kappa, c > 0$

$$\mathcal{E} = \frac{1}{4\pi}\left[\sqrt{4c^2+\kappa^2}(2^2+\kappa^3) - 8c^4 \ln\left(\frac{\kappa}{2c} + \sqrt{\frac{\kappa^2}{4c^2}+1}\right)\right]. \tag{6.3}$$

Assuming $\kappa >> c$

$$\mathcal{E} = \frac{1}{\pi}\left[\frac{\kappa^4}{4} - 2c^4 \ln\left(\frac{\kappa}{c}\right)\right] = \frac{1}{\pi}\left[\frac{\kappa^4}{4} + c^4 \ln\left(\frac{c^2}{\kappa^2}\right)\right]. \tag{6.4}$$

When $N \to 0$ the energy becomes

$$\mathcal{E} = \frac{\kappa^4}{4\pi}. \tag{6.5}$$

We will consider the energy at $N = 0$ as the ground state energy of the system and thus Eq. (6.5) can safely be ignored, so the final energy density for the 2D condensate becomes

$$\mathcal{E}_{\text{LHY2D}} = \frac{1}{\pi} c^4 \ln\left(\frac{c^2}{\kappa^2}\right). \tag{6.6}$$

Note that this expression is not exactly the same as the one Petrov used [14], but exhibits the dependencies on c in the same manner.

References

[1] S. N. Bose, Z. Physik. **26**, 178 (1924).

[2] A. Einstein, Sitz.ber. Preuss. Akad. Wiss. Phys. **23**, 245 (2006).

[3] K. B. Davis, M. O. Mewes, M. R. Andrews, N. J. van Druten, D. S. Durfee, D. M. Kurn, and W. Ketterle, Phys. Rev. Lett. **75**, 3969 (1995).

[4] E. P. Gross, Nuovo Cimento **20**, 454–477 (1961).

[5] L. P. Pitaevskii, Sov. Phys. JETP **13**, 451 (1961).

[6] A. L. Fetter, Laser Physics **18**, 1–11 (2008).

[7] T. D. Lee, K. Huang, and C. N. Yang, Phys. Rev. **106**, 1135 (1957).

[8] I. Ferrier-Barbut, Physics Today **72**, 46 (2019).

[9] D. S. Petrov, Phys. Rev. Lett. **115**, 155302 (2015).

[10] C. R. Cabrera, L. Tanzi, J. Sanz, B. Naylor, P. Thomas, P. Cheiney, and L. Tarruell, Science **359**, 301–304 (2018).

[11] G. Semeghini, G. Ferioli, L. Masi, C. Mazzinghi, L. Wolswijk, F. Minardi, M. Modugno, G. Modugno, M. Inguscio, and M. Fattori, Phys. Rev. Lett. **120**, 235301 (2018).

[12] N. B. Jørgensen, G. M. Bruun, and J. J. Arlt, Phys. Rev. Lett. **121**, 173403 (2018).

[13] T. G. Skov, M. G. Skou, N. B. Jørgensen, and J. J. Arlt, Phys. Rev. Lett. **126**, 230404 (2021).

[14] D. S. Petrov and G. E. Astrakharchik, Phys. Rev. Lett. **117**, 100401 (2016).

[15] C. J. Pethick and H. Smith, *Bose-Einstein condensation in dilute gases.* (Cambridge University Press).

[16] I. Ford, *Statistical physics, An entropic approach* (2013).

[17] F. Dalfovo, S. Giorgini, L. P. Pitaevskii, and S. Stringari, Rev. Mod. Phys. **71**, 463 (1999).

[18] S. Bargi, *Vortices and Persistent Currents in Rotating Bose Gases. A diagonalization approach*, Ph.D. thesis, Lund University (2010).

[19] M. Ota and G. E. Astrakharchik, SciPost Phys. **9**, 20 (2020).

[20] D. M. Larsen, Annals of Physics **24**, 89 (1963).

[21] P. J. Bendt, Phys. Rev. **127**, 1441 (1962).

[22] J. D. Reppy and D. Depatie, Phys. Rev. Lett. **12**, 187 (1964).

[23] Y. Li, Z. Chen, Z. Luo, C. Huang, H. Tan, W. Pang, and B. A. Malomed, Phys. Rev. A **98**, 063602 (2018).

[24] K. P. G. Xie Shuangquan and K. Theodore Proc. R. Soc. A.4742017055320170553 (2018).

[25] B. Chatterjee, Exploring vortex formation in rotating bose-einstein condensates beyond mean-field regime (2022).

[26] J.-k. Kim and A. L. Fetter, Phys. Rev. A **72**, 023619 (2005).

[27] M. N. Tengstrand, P. Stürmer, E. O. Karabulut, and S. M. Reimann, Phys. Rev. Lett. **123**, 160405 (2019).

[28] J. J. Sakurai and J. Napolitano, *Modern quantum mechanics*, 3rd ed. (2021) pp. 94–95.

[29] M. N. Tengstrand, *Superfluidity and Supersolidity in Ultracold Atomic Gases Beyond Mean Field*, Ph.D. thesis, Lund University (2022).

[30] J. Polo, R. Dubessy, P. Pedri, H. Perrin, and A. Minguzzi, Phys. Rev. Lett. **123**, 195301 (2019).

[31] F. Bloch, Phys. Rev. A **7**, 2187 (1973).

[32] X. Liu and J. Zeng, One-dimensional purely lee-huang-yang fluids dominated by quantum fluctuations in two-component bose-einstein condensates (2021).

[33] S. A. Chin and E. Krotscheck, Phys. Rev. E **72**, 036705 (2005).